New Materials by Mechanical Alloying Techniques

E. Arzt and L. Schultz
Editors

INFORMATIONSGESELLSCHAFT · VERLAG

ISBN 3-88355-133-3

Papers presented at the DGM Conference
"New Materials by Mechanical Alloying Techniques",
Calw-Hirsau (FRG), October, 1988
under the direction of
Dr. E. Arzt, Stuttgart and Dr. L. Schultz, Erlangen.

Printed in Germany

Analysis and Modelling of the Creep-Fatigue Behaviour of Oxide Dispersion Strengthened Superalloys

D. M. Elzey and E. Arzt, Max-Planck Institut für Metallforschung, Stuttgart

Abstract

The creep-fatigue behaviour of two representative, commercial ODS (Oxide Dispersion-Strengthened) superalloys, Inconel MA 754 and MA 6000, both of which are produced by mechanical alloying, has been investigated. The mechanisms leading to failure are identified and discussed with particular emphasis on creep-fatigue interaction phenomena. Fine-grain regions are found to be the primary source of crack-initiation by the formation of creep damage. A finite difference approach to modelling of these damage processes is introduced. Results of the model are compared with experimentally determined crack initiation life. In order to explain waveform effects it is suggested that, in analogy with prestraining experiments, rapid plastic deformation can introduce residual stresses in the neighbourhood of hard particles such as oxide dispersoids during asymmetric creep-fatigue cycling. Subsequent creep damage rates are thus strongly influenced by the magnitude, sign and rate of prior plastic straining.

Introduction

The exceptional creep properties of dispersion strengthened alloys produced by mechanical alloying have resulted in extensive study of their creep behaviour. As a consequence, our understanding of creep-related phenomena in these materials is now comparable with that of currently-used, non-dispersion strengthened alloys (1). However, the high temperature fatigue behaviour of dispersion strengthened alloys has received relatively little attention although this aspect may well turn out to be design-limiting for potential applications. The current study concerns creep-fatigue of two commercially available ODS superalloys. Some results have already been presented and discussed in a previous paper (2) and are therefore only briefly reviewed here.

With increasing temperature and decreasing cyclic frequency, fatigue life will be determined by some combination of cycle-dependent and time-dependent damage processes. Complete evaluation of the mechanisms leading to failure requires consideration of the influences of one type of damage on another. These creep-fatigue interactions are frequently reflected in the effect of intergranular cavities on fatigue crack initiation and growth rates or the effect of cyclic plastic deformation on cavity nucleation and growth rates. An important consideration which is often overlooked when analyzing creep-fatigue behaviour is the state of stress produced by rapid plastic deformation and its influence on subsequent creep damage. It will be demonstrated in this paper that such considerations are necessary in order to explain the strong influence of cyclic waveform on creep-fatigue life.

Experimental

Present experimental work has been concentrated on the two yttrium-oxide dispersion-strengthened superalloys Inconel MA 754 and MA 6000. Both alloys are produced by INCO Alloys International, by the mechanical alloying process (3). Compositions and microstructural data are summarized in table 1.

MA 754 is strengthened by solid solution and by the dispersion. In addition, an elongated grain structure is obtained during heat treatment (see ref. 4 for a more detailed description of the microstructure). MA 6000 is strengthened at intermediate temperatures by γ'-$Ni_3(Al,Ti)$ precipitates while at temperatures above 900 °C the dispersion becomes the dominant source of strength. A bi-modal distribution of grain sizes exists in MA 6000; large grains with lengths on the order of several centimeters and grain aspect ratios (GAR) > 20 account for some 95% of the volume, while the remainder comprises a distribution of much smaller grains with lengths ranging from 100 μm to several millimeters and GAR between 1 and 20. For a more detailed description of the microstructure of MA 6000 the reader is referred to (5,6).

Creep-fatigue tests using total strain control have been carried out at 850, 950 and 1050 °C. Cycle forms included tensile hold-times (H-T), slow tensile loading followed by fast compression, commonly referred to as 'slow-fast' (S-F) and slow symmetric (S-S). Samples from tests run to physical separation of the specimen as well as interrupted experiments were then subjected to optical, scanning electron and transmission electron microscopy. Further experimental details will be given elsewhere (7).

Table 1. Elemental Composition of Materials and Microstructural Data

Alloy	Ni	Cr	Fe	Al	Ti	W	Mo	Co	Ta	C	B	Zr	Nb	Y_2O_3
MA 6000	Bal	15.5	-	4.5	2.5	3.8	2.0	-	1.9	.06	.01	.16	-	1.08
MA 754	Bal	20.5	.13	.30	.35	-	-	-	-	.06	-	-	-	0.5

	Grain Size [mm]	GAR	Particle Dia [nm]	Particle Spac [nm]	Texture
MA 6000	4-10	20	30	150	<110>
MA 754	0.5-3.0	10	15	125	<100>

Results

Examination of the creep-fatigue fracture behaviour of MA 6000 and MA 754 has provided ample evidence that crack initiation is caused by the presence of grain structure inhomogeneities in the form of fine grains (see also ref. 2). This is illustrated by figure 1, which shows a polished and etched axial section of an MA 6000 specimen tested to failure in 735 cycles. A crack has initiated at the transverse boundary between two fine grains and has propagated radially outward into the surrounding macrograin. Figure 2 represents a fracture surface in which more than 25 internal crack initiation sites could be identified.

Interrupted tests have shown that the transverse boundaries of fine grains are subject to cavitation damage. As typified by figure 3, cavities have an elliptical shape and range in size from 1-2 μm just prior to coalescence.

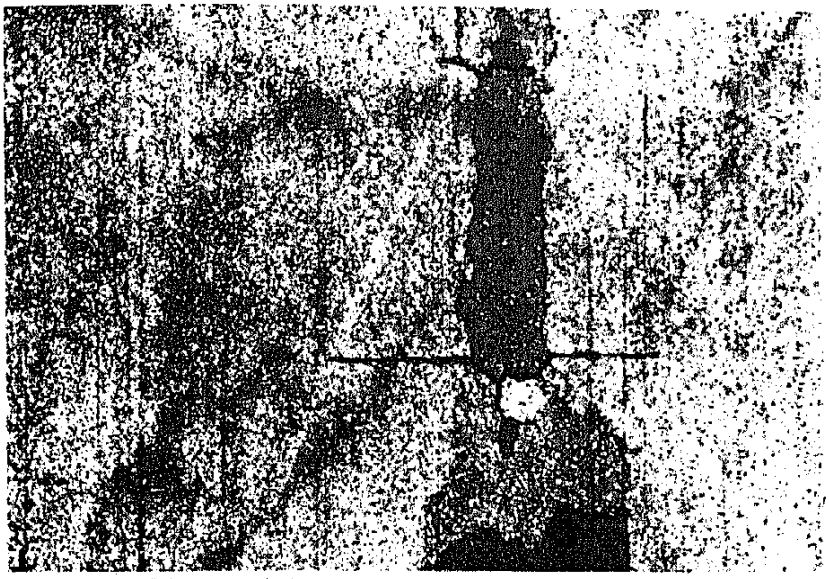

Fig.1.
Crack initiate internally at fine grains during creep-fatigue.(MA 6000, etched and polished axial section, 850°C, slow-fast, $\dot{\epsilon}_S = 10^{-5}[s^{-1}]$, $\dot{\epsilon}_F = 10^{-2}[s^{-1}]$, failure after 242 cycles)

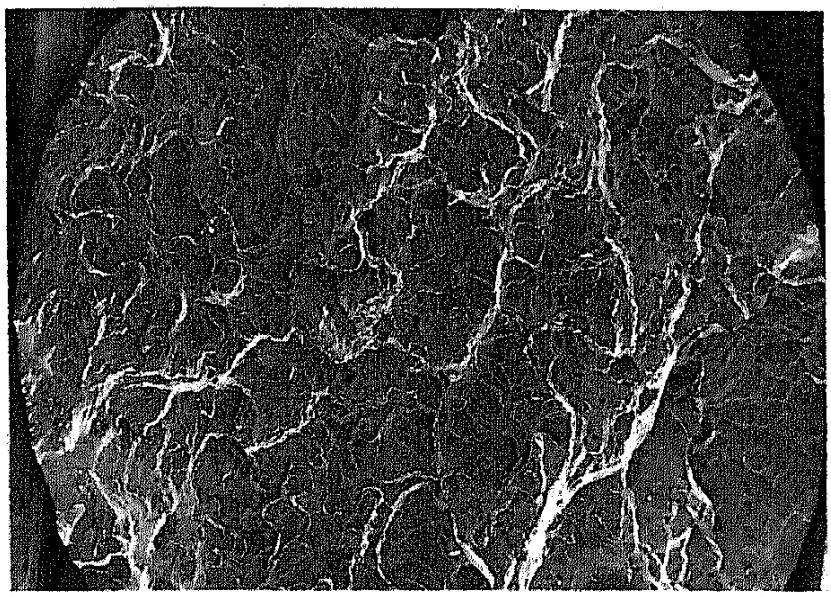

Fig.2.
Fracture surface of a sample tested under 'slow-fast' conditions at 850°C. More than 25 individual crack initiation sites may be identified. (MA 6000, $\dot{\epsilon}_S = 10^{-5}[s^{-1}]$, $\dot{\epsilon}_F = 10^{-2}[s^{-1}]$, $\Delta\epsilon/2 = 0.3\%$, failure after 242 cycles)

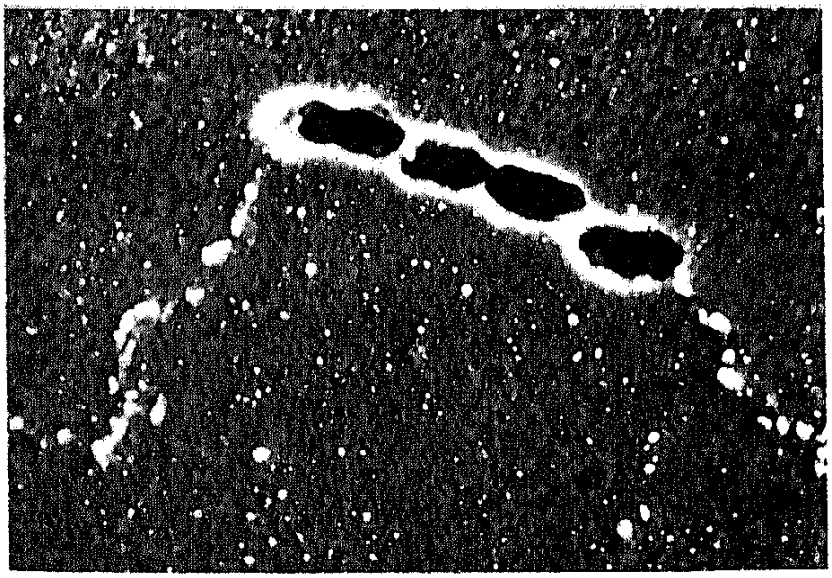

Fig 3.
Cavitation of the transverse boundary of a fine, included grain. Pores are typically 1–2 μm wide at coalescence and are elliptical in shape. (MA 6000, slow-fast, 850 °C, $\dot{\epsilon}_S = 10^{-5}$ [s^{-1}], $\dot{\epsilon}_F = 10^{-2}$ [s^{-1}], interrupted after 420 cycles)

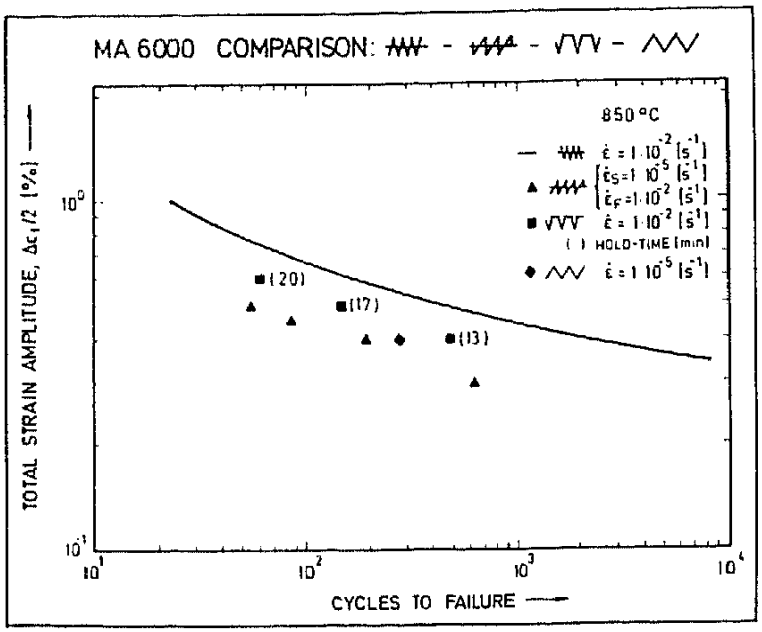

Fig.4.
Results of creep-fatigue tests of MA 6000 at 850°C illustrate the influence of waveform on cyclic life.

Figure 4 illustrates the effect of waveform on cyclic life of MA 6000 at 850 °C. It may be seen that the S-F cycle results in the shortest life, followed by S-S and H-T cycles. Results of symmetric fatigue cycling at a strain rate of 10^{-2} [s^{-1}] are also shown for comparison.

Although cracks were found to initiate internally at grain defects under all creep-fatigue conditions tested, metallographic examination often revealed features distinguishing one waveform from another. It was found for example that during tensile hold-time tests, spherical pores occur frequently on grain boundaries parallel to the loading axis and occasionally, also within the matrix. Pores not lying on a grain boundary appear to be associated with larger yttrium-aluminate particles. During S-F and S-S cycling, pores were found only on transverse grain boundaries. It was also observed that cracks initiating during tensile hold-time tests display a greater tendency to propagate intergranularly along longitudinal fine grain

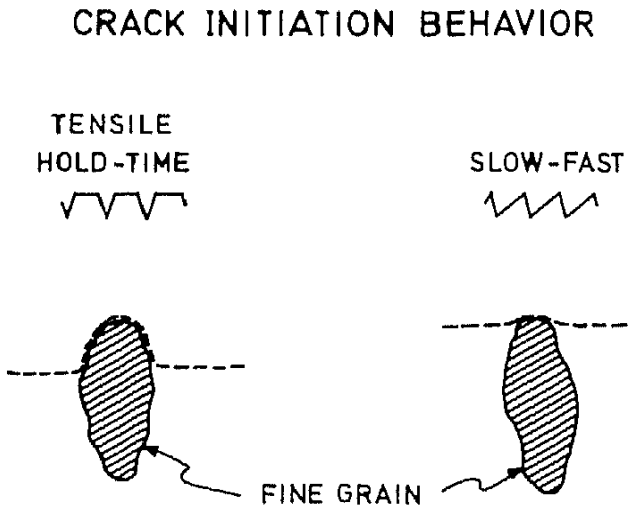

Fig.5.
During tensile hold-time cycling, cracks tend to propagate along boundaries parallel with the stress axis before extending transgranularly into the surrounding matrix.

provides further confirmation that creep-fatigue life and the influence of waveform are being largely determined by local residual stresses.

Enhanced recovery at high temperatures will prevent the buildup of residual stresses as large as those produced during room temperature deformation, but it seems very likely that their effect may be significant. Residual stresses produced during RT prestraining have been found to persist over a significant fraction of creep life (9). Alloys containing oxide particles and/or grain boundary carbides and which fail or initiate cracks by intergranular cavitation, may be expected to exhibit a similar influence of waveform on creep-fatigue life.

Creep-Fatigue Crack Initiation Model

The following is a brief description of a model which has been developed in an attempt to quantify the mechanism leading to creep-fatigue crack initiation. The development has been tailored to the physical situation encountered in ODS superalloys: cracks initiate by cavity growth and coalescence on isolated, transverse grain boundaries. For a more detailed description, the reader is referred to an upcoming publication (7).

Cavity growth models have been successfully applied to a number of alloys evaluated under conditions of constant stress, but little work has been done to apply these concepts to situations wherein the applied stress continually varies. Analytical approaches based on creep models where a time-averaged stress during a creep-fatigue cycle is used, cannot be expected to reflect the influence of waveform; S-F cycles generally have a lower time-averaged tensile stress than an H-T cycle of identical stress amplitude, yet the S-F cycle is considerably more damaging. Instead, a finite difference approach is found to be more suitable since the damage can be integrated over time as a function of stress.

The stresses which act across the grain boundary in question are generally not the same as the externally applied stress because of load shedding to the surrounding grains and local relaxation of elastic stresses. Load shedding is accounted for by a compatibility condition requiring grain boundary displacements not to exceed displacements in the surrounding matrix, unless displacements can be accommodated by elastic stress relaxation. In order to better visualize the process of accommodation by local stress relaxation, consider a penny-shaped crack in an elastically loaded body; the crack opening displacement (which may be calculated by linear elasticity theory) is made possible by the relaxation of elastic stresses near the crack faces. Analogously, the grain boundary 'opens' as displacements due to cavitation occur and this opening may be accommodated by stress relaxation. The calculation of the grain boundary stress σ_{gb} is then determined as a balance between an increment in the applied stress and an increment of relaxed stress, i.e., $\sigma_{gb} = \sigma_{gb} + \Delta\sigma_a - \Delta\sigma_{rel}$.

Once the grain boundary stress is known for a given time increment, the change in pore radius ΔR under the influence of this stress may be calculated. The mechanisms of pore growth which are considered include grain boundary diffusion, for which ΔR may be written as (13,14)

$$\Delta R = \frac{2\ \Omega\ \delta D_b}{kT\ \lambda\ Q(\omega)\ R} \cdot \sigma_{gb} \cdot \Delta t \qquad (1)$$

and plastic hole growth, for which ΔR may be written as (15)

$$\Delta R = 0.6\ B\ \frac{\lambda^2}{B} \cdot \frac{1}{R}\left[\frac{1}{(1-\omega)^n} - (1-\omega)\right](\sigma_{gb} - \sigma_{th})^n \cdot \Delta t \qquad (2)$$

where the effect of a pseudo-threshold stress σ_{th} for creep has been included in the latter expression. The symbols used are defined as follows:

Ω:	atomic volume	R: pore radius
δD_b:	grain boundary diffusion coef.	B: Dorn's constant
k:	Boltzmann's constant	n: stress exponent
T:	absolute temperature	λ: cavity spacing
ω:	cavitated area fraction	$Q(\omega)$: shape factor

Crack initiation is assumed to be completed when the cavitated area fraction ω reaches a critical value of $\omega = 0.7$. The number of cycles to crack initiation predicted by the model is compared with experimental data for S-F tests in figure 6 and with data for H-T tests in figure 7. The model predictions are shown as a scatter band in both figures, which results from using a wide range of material constants and parameters. The scatter band can be shifted laterally by varying the critical area fraction of cavitated boundary.

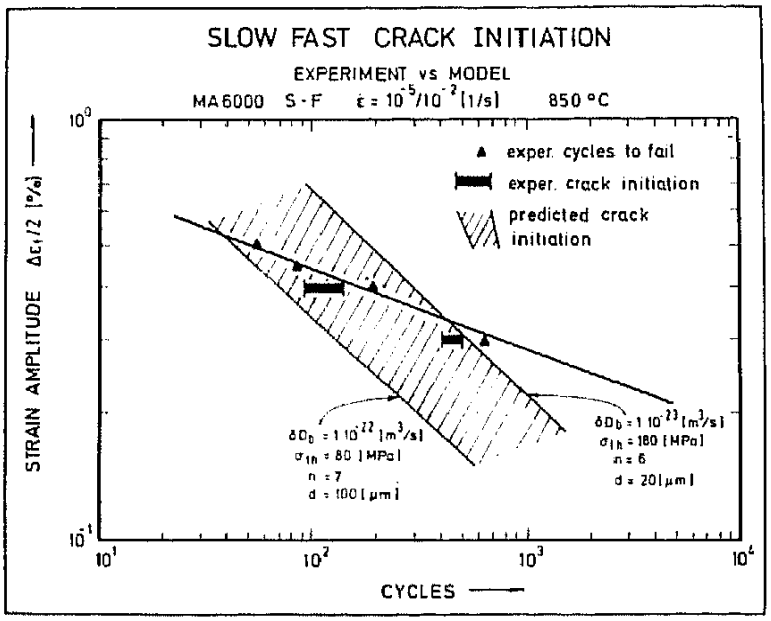

Fig.6.
Comparison of crack initiation life as predicted by the model with experimental data for slow-fast tests.

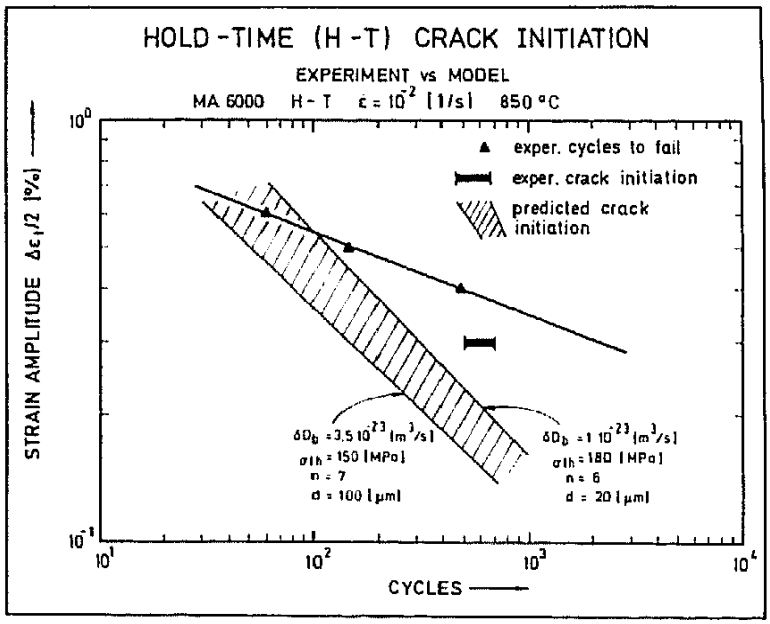

Fig.7.
Comparison of crack initiation life as predicted by the model with experimental data for tensile hold-time tests.

boundaries before extending transgranularly into the surrounding grains. This tendency is illustrated schematically in figure 5 and is compared with behaviour for S-F tests where the intergranular initiation site and transgranular crack growth surface are practically coplanar. Slow-slow tests are characterized by a generally lower density of crack initiation sites in comparison with S-F and H-T tests. Additionally, interrupted S-S tests demonstrated that cavities which nucleate during slow tensile loading may frequently be sintered during slow compression. Sintering did not occur during S-F and H-T tests.

Discussion

The nucleation and diffusional growth of cavities leading to intergranular fracture is a well known phenomenon in creep-resistant, low-alloy steels and superalloys exposed to low stress, high temperature conditions for extended periods. Although cavitation may occur in some materials during high frequency cyclic loading, the nucleation and growth of pores during high temperature fatigue is normally associated with diffusional or dislocation creep. For the case of MA 6000, the presence of precipitate-free zones between cavities and the spherical caps shape of the pores are taken to be indications that creep cavitation is occurring. The particular susceptibility of the boundaries of fine grains to fatigue and cavitation damage has been discussed previously (2). Briefly, fine grains have been found to have crystallographic orientations which may be very different than the highly textured <110> orientation shared by normally recrystallized macrograins. Thus, some fine grains will exhibit a significantly higher elastic modulus in the loading direction with the result that transverse boundaries are subjected to correspondingly higher stresses.

As for a variety of other alloys, including Al-5Mg (10), stainless steels (e.g. 11) and superalloys (e.g. 12), the S-F cycleform has proven to be the most damaging for MA 6000 (see fig. 4). The initiation of cracks also occurs most quickly during slow-fast cycling, as has been demonstrated by comparison of interrupted tests. This behaviour may be explained by considering the effect of local residual stresses. The rate of creep damage accumulation during the slow tensile portion of the cycle will depend on the local stress state existing at the start of creep loading. The local stress state depends, in turn, on the amplitude, sign and rate of the preceding plastic deformation. Studies of the effect of prestraining on subsequent creep damage rates demonstrates this point well: It has been shown that creep life is greatly reduced if prestraining is done in compression, while tensile prestraining is seen to exert little influence on subsequent creep life (8,9). This phenomenon is due to local residual stresses resulting from the plastic deformation of matrix material in the neighborhood of very hard particles such as oxides or carbides. Compressive prestraining results in residual stresses which complement the applied tensile stress. Thus, cavities which nucleate on grain boundaries transverse to the applied stress experience accelerated growth and coalescence. On the other hand, tensile prestraining induces a residual stress state which tends to oppose a tensile (creep) stress and so cavities on transverse boundaries may experience inhibited growth. It has been observed in fact, that tensile prestraining enhances growth of pores on grain boundaries parallel to the stress axis. It is to be expected that residual stresses created by rapid plastic straining exert a similar influence on creep damage rates during creep-fatigue loading.

Thus, two preconditions must be satisfied for residual stresses to be a significant influence during creep-fatigue; (1) the material must contain non-deforming inclusions (on grain boundaries to affect damage rate due to cavitation) and, (2) sufficient plastic deformation must occur athermally in the matrix surrounding the hard particle. In MA 6000 and MA 754, larger oxide dispersoids and yttrium-aluminate particles lying on or near grain boundaries are available to act as stress concentrations and as cavity nuclei. During H-T cycling, creep follows rapid tensile deformation which, in analogy with tensile prestraining tests, would be expected to promote cavitation on boundaries parallel with the stress axis while exerting little or no influence on the growth of pores on transverse boundaries. That this is indeed observed

The comparison of prediction with experiment in figures 6 and 7 is encouraging as order-of-magnitude agreement is found; this makes it plausible that crack initiation does indeed occur by a creep damage mechanism. However, two inadequacies are apparent in the model; firstly, the predicted curves are too insensitive to the strain amplitude, (i.e., curves are too steep), and secondly, although the prediction is acceptable for the S-F case, the influence of waveform is not properly accounted for in going to the H-T cycle.

The insensitivity of the prediction to cyclic strain amplitude is a consequence of the stress-based approach taken for modelling the damage rate. The cyclic plastic deformation, which is conventionally expressed as a function of the inelastic strain range $\Delta\epsilon_{pl}$, must be incorporated into the damage rate equation. The inability of the model to accurately predict the influence of waveform could be improved by including the influence of prior plastic deformation on creep damage rate. This aspect is currently being investigated by considering a residual stress term which is added to the grain boundary stress. The residual stress term depends on the loading prior to creep and is a function of strain amplitude, loading direction and strain rate. It must also be a function of time since recovery processes due to creep are occurring.

Summary

The creep-fatigue behaviour of the two ODS alloys MA 6000 and MA 754 has been investigated. Failure is found to occur in both alloys as a result of cracks which initiate at grain structure defects. These defects, which occur primarily in the form of fine, included grains, are susceptible to intergranular cavitation. Cracks thus initiated grow transgranularly and eventually coalesce, leading to fracture. Since this initiation process is found to take up a significant portion of the number of cycles to failure, its understanding and eventual suppression may be of great practical importance.

Investigation of the influence of waveform on the creep-fatigue life has shown the slow-fast waveform to be most damaging, followed by slow-slow and tensile hold-time cycles. The principal effect of waveform on cyclic life is ascribed to the influence of local residual stresses produced during rapid plastic deformation on subsequent creep damage rates. Matrix plastic deformation in the vicinity of non-shearable particles such as oxide dispersoids results in a localized stress state which may either accelerate or inhibit cavity growth, depending on the direction (compressive → accelerates; tensile → inhibits) of prior plastic straining. The occurrence of cavitation on grain boundaries parallel with the loading axis during H-T tests could also be rationalized by the presence of residual stresses.

A model for the simulation of the damage processes leading to crack initiation during creep-fatigue of ODS superalloys has been introduced. While able to predict crack initiation during S-F cycling at lower strain amplitudes, the current model fails to properly reflect the influence of waveform. Further work is being concentrated on the introduction of a means to include the influence of residual stresses on creep damage rates.

Acknowledgements

The authors are especially grateful to C. Weis for assistance with SEM studies and special metallography. Parts of this work have been carried out within the frame of the European Collaborative Programme COST 501. We would like to acknowledge the financial support of the Bundesministerium für Forschung und Technologie in the Federal Republic of Germany under project number O3ZYK1228.

References

(1) E. Arzt, this volume.
(2) D.M. Elzey, E. Arzt in: Superalloys 1988, S. Reichman et al, eds., The Metallurgical Society, 1988, pp.595-604.
(3) G.A.J. Hack in: Frontiers of High Temp Materials II, J.S. Benjamin and R.C. Benn, eds., (USA: INCO Alloys International, 1983), pp.3-18.
(4) J.J. Stephens, W.D. Nix: Met Trans 16 (1985) 1307.
(5) J. Schröder in: Fortschr.-Ber. VDI, Reihe 5 (1987), Nr.131.
(6) H. Zeizinger in: Fortschr.-Ber. VDI, Reihe 5 (1987), Nr.121.
(7) D.M. Elzey: Ph.D. Thesis, Univ of Stuttgart, 1988, to be published.
(8) B.F. Dyson, M.F. Loveday, and M.J. Rodgers: Proc. R. Soc. A 349 (1976) 245.
(9) K. Shiozawa, J.R. Weertman: Acta Met 31 (1982) 993.
(10) S. Baik, R. Raj: Met Trans 13A (1982) 1215.
(11) S. Majumdar, P.S. Maiya: Canad. Metall. Quart. 18 (1979) 57.
(12) M.Y. Nazmy: Met Trans 14A (1983) 449.
(13) D. Hull, D.E. Rimmer: Phil. Mag. 4 (1959) 673.
(14) M.V. Speight, J.E. Harris: Metal Sci. J. 1 (1967) 83.
(15) A.C.F. Cocks, M.F. Ashby: Prog. Mat. Sci. 27 (1982) 189.